Electron Beam Emission from a Diamond-Amplifier Cathode

Xiangyun Chang,[1] Qiong Wu,[1] Ilan Ben-Zvi,[1] Andrew Burrill,[1] Jorg Kewisch,[1] Triveni Rao,[1] John Smedley,[1] Erdong Wang,[1] Erik M. Muller,[2] Richard Busby,[3] and Dimitre Dimitrov[3]

[1]*Brookhaven National Laboratory, Upton, New York 11973, USA*
[2]*Stony Brook University, Stony Brook, New York 11794, USA*
[3]*Tech-X Corporation, 5621 Arapahoe Avenue Suite A, Boulder, Colorado 80303, USA*

(Received 11 March 2010; published 15 October 2010)

The diamond amplifier (DA) is a new device for generating high-current, high-brightness electron beams. Our transmission-mode tests show that, with single-crystal, high-purity diamonds, the peak current density is greater than 400 mA/mm^2, while its average density can be more than 100 mA/mm^2. The gain of the primary electrons easily exceeds 200, and is independent of their density within the practical range of DA applications. We observed the electron emission. The maximum emission gain measured was 40, and the bunch charge was 50 pC/0.5 mm^2. There was a 35% probability of the emission of an electron from the hydrogenated surface in our tests. We identified a mechanism of slow charging of the diamond due to thermal ionization of surface states that cancels the applied field within it. We also demonstrated that a hydrogenated diamond is extremely robust.

DOI: 10.1103/PhysRevLett.105.164801 PACS numbers: 29.25.Bx

Many modern science applications, such as ultra-high-power free-electron lasers (FELs) [1,2], Energy-recovery linac (ERL) light sources [3,4], and electron cooling of hadron accelerators [5] require high average-current, high-brightness electron beams. Traditional cathodes for high-brightness rf injectors are metallic photocathodes or semiconductor photocathodes. The former has a low quantum efficiency (QE) of 10^{-3} or less, and a relatively high emittance compared to that of a semiconductor photocathode, making it hard to realize high average-current, high-brightness electron beams. Semiconductor photocathodes have a higher QE (a few percent) and lower emittance (~ 0.1 eV thermal energy on cathode surface), but have very short lifetimes. In contrast, the diamond amplifier (DA) we proposed a few years ago [6,7] generates high-average-current, high-brightness electron beams with a very long lifetime.

Figure 1 shows that one surface of the diamond window is coated with metal, while the other is hydrogenated. Hydrogen termination confers a negative electron affinity (NEA) on the diamond's surface [8]. A photocathode, such as magnesium, generates primary electrons that are accelerated to about 10 keV by a dc voltage. These primary electrons penetrate the coating, and produce one *e-h* pair for every 13.3 eV energy of the primary electron [9]. Then, the rf field with the right phase separates the electrons and holes. The holes drift back to the metal and are absorbed, while the electrons move through the diamond and are emitted from its hydrogenated NEA surface (the *H* surface). Consequently, one high energy primary electron yields a few hundred low-energy secondary electrons.

The primary electrons do not determine the characteristics of the electron beam; rather, it is the secondary electrons that are produced by energetic primary electrons, and rapidly thermalized (in $\sim$100 fs) within the diamond's lattice. The excellent thermal conductivity of the diamond ensures that the DA can handle a very large current density. Our simulations [10], confirmed experimentally [11], show that a modest diamond of 1 cm diameter can deliver average currents approaching the ampere level. Modeling showed that the thermal energy of the secondary electrons as they travel in the diamond is about 0.026 to 0.046 eV for applied fields from 0.05 to 1 MV/m [12]. However, the emission from the *H* surface of the DA can entail an increase in thermal emittance; this is the subject of our current studies.

The lifetime of DA will be very long because once the surface of the diamond is hydrogenated, the hydrogen atoms form strong stable chemical bonds with the carbon atoms. Upon exposure to air, the *H* surface might attract molecules, such as water, but, after heating the sample above 200 °C, water desorbs from the surface without degrading the quality of hydrogenation [13]. The mobility of the electrons and holes in the diamond is about 2000 cm^2/V s at room temperature; their saturated drift velocity is about 1.5×10^7 cm/s [12], and relatively independent of temperature. These properties, viz., high

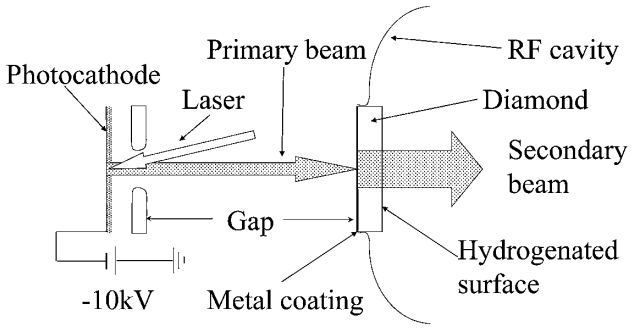

FIG. 1. DA in a rf cavity. The gap between the photocathode exit and the metal coating is roughly 5 cm.

mobility and saturated drift velocity, support the usage of the DA in rf cavities.

We studied the DA in two stages. In the first stage, the transmission-mode measurement (Fig. 2), the NEA surface was replaced by 40 nm Ti/Pt coating, that does not emit electrons. In the transmission-mode measurements, we studied the properties of the secondary-electron generation and transmission in the diamond. In the second stage, the emission-mode measurement (Fig. 4), the sample was hydrogen terminated to allow electron emission.

The transmission-mode measurements were carried out on three types of diamonds: Single-crystal type IIA natural diamonds, synthetic high-purity polycrystalline diamonds, and, synthetic high-purity single-crystal diamonds, the last of which we found was the only one suitable for use as the DA. Natural diamonds are unsuitable because they contain high levels of impurities, and hence, trap more electrons in the bulk than do high-purity synthetic diamonds. Similarly, polycrystalline diamonds trap electrons and holes at grain boundaries [14]. The transmission gain is defined as the ratio of the collected current to the primary-electron current. The *e-h* pairs are created in a thin layer on the entrance surface and the bulk trapping was negligible in our samples. So, the transmission gain only depends on the primary electrons' energy and the electric field. The symbols connected by the solid lines in Fig. 3 represent the primary-electron gain as a function of the electric field for a few primary-electron energies obtained from one of our synthetic high-purity single-crystalline diamonds at room temperature. For comparison, the symbols with dotted lines with the same marker are the results of our simulation using VORPAL to model the generation of *e-h* pairs by primary electrons and their transport in an external field [15].

We measured the primary-electron gain with a primary-electron energies of 4, 5, 6, 7, and 8 keV. The saturation gains of every one of them form a straight line that crosses the primary-energy axis at 3.3 keV, reflecting the electron energy lost in the metal coating. This loss is accounted for in Fig. 3. The slope is 19 eV, i.e., the value of the average energy of the primary electrons required to generate one *e-h* pair in the diamond that is much higher than the reported value of 13.3 eV [9]. We consider that this higher number indicates the loss of secondary electrons due to diffusion near the diamond's surface. The measured slope does not discriminate the loss of electrons before they reach the collection electrodes. By replacing the primary-electron beam with an x-ray beam of different energy and hence, penetration depth, we identified that the predominant mechanism of loss was the absorption of the isotropically diffusing secondary electrons at the input surface [9]. We also demonstrated in these x-ray measurements that this type of diamond can deliver up to an average-current density more than 100 mA/mm^2. The 1 ns long x-ray bunches, generated at the National Synchrotron Light Source, produced pulses of current in the diamond with a sub-ns rise and a 5 ns fall, The latter was caused by the drift time of *e-h* pairs, created throughout our 500 μm thick diamond by x rays. This artifact is not relevant to the application of DA with primary electrons. The peak current density in our experiment was greater than 400 mA/mm^2 [11].

Another important observation is that the gain is independent of the density of primary electrons in the practical range of DA applications [16]. This finding reflects the dimension of the secondary-charge cloud, viz., about a few hundred nm, and hence, for primary-current densities less than 10 mA/mm^2, the clouds from individual primary electrons do not overlap, and so the gain curve is independent of charge density. Accordingly, a single primary-electron model effectively describes the plasma-separation process [15]. This value of 10 mA/mm^2 is enough for most applications that require an ultra-high-current density.

Figure 4 is a scheme of the emission-mode measurements. The samples were hydrogenated on one side (the *H* surface), and metal-coated on the other side. The hydrogenation procedure was as follows: Samples were heated to about 800 °C in a vacuum for half an hour, after which we considered that the diamond surface was bare [17]. Next, we exposed the samples for an hour to a flow of hydrogen atoms generated by a commercially atomic hydrogen source. Thereafter, the opposite side of each sample was metal-coated with 15 nm of Ti, followed by 25 nm of Pt. We measured electron emission in ultrahigh vacuum of 1×10^{-9} Torr. There is a gap of 200 to 500 μm between the anode and the *H* surface. The applied high voltage

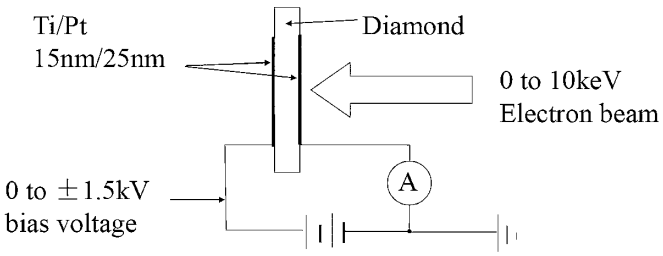

FIG. 2. Transmission-mode measurement. Diamond thickness: 0.15–0.3 mm.

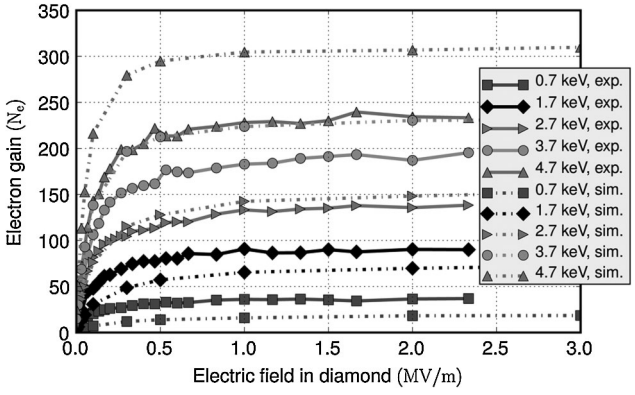

FIG. 3. Gain curve of a synthetic high-purity single-crystalline diamond. Solid lines are the experiment results and dotted lines are the simulation results. A comparison shows overall qualitative agreement.

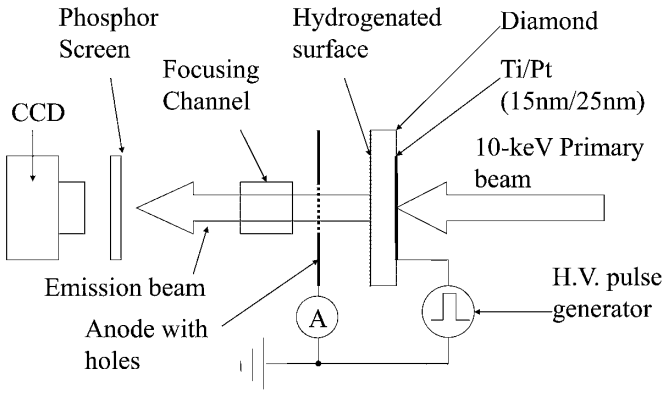

FIG. 4. Emission-mode measurement. The effective primary-electron voltage is 10 kV minus the HV pulse voltage.

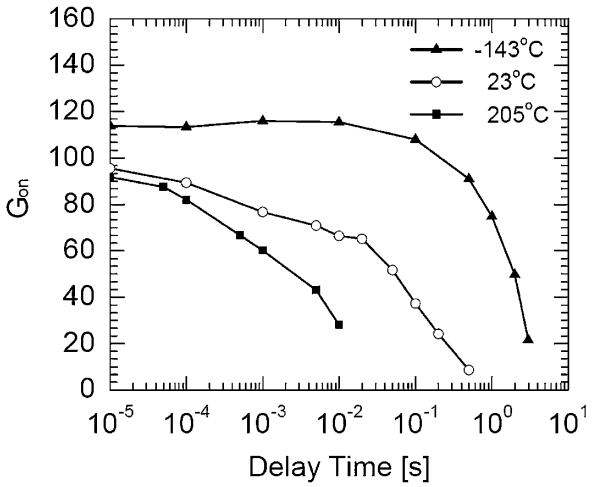

FIG. 5. G_{on} vs delay time at various temperatures due to dc shielding.

(HV) between the anode and metalized surface of the diamond generates a field in the diamond and across the gap towards which the electrons emitted from the diamond are accelerated. Part of the electron beam emerges from the apertures in the anode, and then is focused electrically before it hits the phosphor screen. We obtained the average value of the emission current by measuring the integrated anode current. The fraction of the beam passing through the anode apertures usually is small, and is reduced further by moving the primary beam's spot away from the apertures. An electrometer grounds the anode; thus, the phosphor screen and the anode are at the same potential.

Some dangling bonds and impurities inevitably remain on the H surface. In the presence of an external field, they may become activated thermally to generate excess charge. The density of this charge increases with rising temperature; it builds up over time on the H surface and shields the external field, such that the field inside the diamond declines correspondingly. This process continues until the external field is shielded completely, or all the dangling bonds and impurities are activated. The shielding process is very effective, even when the density of the dangling bonds and the impurities on the H surface is very small. For example, assuming 0.1% coverage of fully activated dangling bonds and impurities, this is enough to shield an external field as high as a few hundred MV/m. In other words, even without the primary electrons, practically any external field is shielded completely in a short time. This was the major reason why we did not obtain good emissions in our early measurements where we always applied a dc field, our so-called dc shielding.

We designed a circuit that accurately controls the delay time between the turn-on time of the high voltage, and the onset of the primary beam. Then, we measured the secondary-electron gain at the beginning of the primary beam pulse (G_{on}) as a function of this delay. G_{on} is the ratio of the measured current to primary current. It overestimates the actual emission gain because the secondary electrons stopped at the H surface also contribute to the current signal due to their passage in the diamond. In these experiments, we used the primary-electron beam as the sensor of the electric field in the diamond.

Figure 5 shows that G_{on} decreases as the delay time increases due to the dc shielding. At lower temperatures, G_{on} remains constant longer because then the ionization rate is slower, and accordingly, the effect of the dc shielding slows down. In principle, this measurement determines the density of holes on the H surface at a particular temperature; therefore, it offers a measure of the quality of hydrogenation.

dc shielding is a relatively slow process. As Fig. 5 shows, for 0.3 MV/m of external field at room temperature, after milliseconds of delay, the G_{on} drops to 90% of its peak value. A higher external field, lower temperature, or shorter delay can reduce dc shielding. For example, as depicted in Fig. 5, if the delay time is less than 100 μs, we can ignore this effect.

Based on this understanding, we designed a pulsed HV circuit, that allows the diamond's self-neutralization during each pulse interval. Figure 6 has the electron-emission images obtained from the phosphor screen for one of our

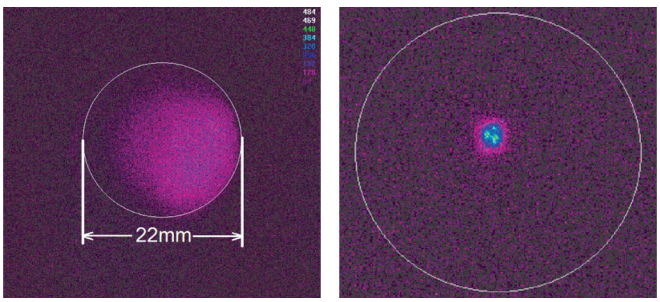

FIG. 6 (color). Images of the electron beam on the phosphor screen. Left: No focusing, primary current is $I_{Pri} = 300$ nA, repetition frequency is 1 kHz, HV pulse width is 10 μs, HV amplitude is -3 kV. Right: With focusing, reduced I_{Pri}. The small bright dots on the right-hand side image are the images of the apertures in the anode.

samples, a $4 \times 4 \times 0.3$ mm^3 synthetic high-purity single-crystal diamond (Element Six).

Undoubtedly, the probability of trapping electrons on the H surface, the gain, and the limit on bunch-charge depend on the quality of hydrogenation. We measured these parameters in our samples under our current conditions. To assess trapping probability, first we accurately controlled the voltage amplitude, the pulse width, and the repetition frequency, and then determined the primary-electron current, which is a continuous wave. An integration circuit recorded the average emission current. Calculating the emission gain during the HV pulse under a known duty cycle is straightforward. Having determined the average emission gain in a pulse, we compared it to the gain data from the transmission-mode measurements to derive the average electron-emission probability in a pulse.

Figure 7 shows our data on the average emission probability; clearly, the emission probability rises as the width of the high-voltage pulse declines. This relationship indicates that most of the emission is concentrated in a short time ($\ll 1$ μs) at the beginning of the pulse. The highest emission probability in our experiment was about 35%, and the peak gain was about 40 at a high-voltage pulse width of 200 ns under a field of 2.7 MV/m.

The bunch charge in our test was the product of the average current and the period of one HV pulse, e.g., 50 pC on an area of roughly 0.5 mm^2 for gates >10 μs.

We cannot assess the limit on emission current density until we can test the device in an rf cavity. We measured more than 20 μA/mm^2 emission current under our present experimental conditions.

The DA proved to be extremely robust. We exposed the hydrogenated diamond samples to air for about half an hour before we installed them in the test chamber, and pumped the chamber down. We obtained good results as we have discussed. There was no degradation in the emission of one sample, exposed to air for a week; later, after exposing it to air for six months, we recorded only a drop of about 50%. This long lifetime probably reflects the strong, stable chemical bonds between the hydrogen atoms and the carbon atoms.

From transmission-mode measurements of the diamond with electrons and with x rays, we found that only the synthetic high-purity single-crystal diamond is suitable for a DA. The peak current density is greater than 400 mA/mm^2 and the average-current density can reach above 100 mA/mm^2; the gain of the primary electrons easily is more than 200, and is independent of the primary electrons density in the practical range of the DA applications. We observed, for the first time, the phosphor-screen image of the electron beam emitted from a diamond-amplified cathode. We proposed the existence of an H-surface electron trapping mechanism. Following this model, we measured the probability of emission as about 35% in one of our samples; expectedly this probability will be higher for pulses shorter than our equipment currently permits. The maximum bunch charge we measured was about 50 pC on an area of about 0.5 mm^2. The maximum emission gain in our present conditions is ~40. Our experiments also verified the DA's powerful characteristics, its extreme robustness, and its potentially bright prospects.

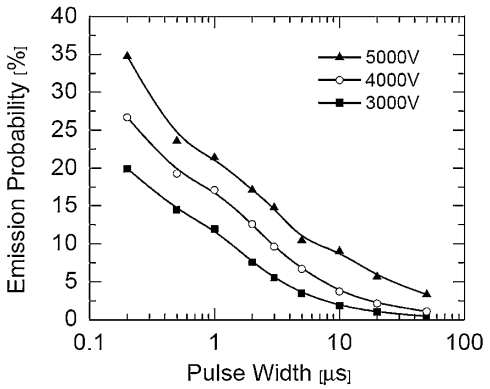

FIG. 7. Average emission probabilities of the secondary electrons 3, 4, and 5 kV correspond, respectively, to a 1.7, 2.2, and 2.7 MV/m field in the diamond.

We were helped in these experiments by many colleagues; we especially highly appreciate the aid from, and discussions with Joan Yater. This work was supported by Brookhaven Science Associates, LLC under Contracts No. DE-AC02-98CH10886 and DE-FG02-08ER41547 with the U.S. DOE.

[1] D. A. G. Deacon *et al.*, Phys. Rev. Lett. **38**, 892 (1977).
[2] G. R. Neil *et al.*, Phys. Rev. Lett. **84**, 662 (2000).
[3] M. Tigner, Nuovo Cimento **37**, 1228 (1965).
[4] S. M. Gruner *et al.*, Rev. Sci. Instrum. **73**, 1402 (2002).
[5] K. Balewski *et al.*, Nucl. Instrum. Methods Phys. Res., Sect. A **441**, 274 (2000).
[6] I. Ben-Zvi *et al.*, Technical Report No. 149, Brookhaven National Laboratory, Upton, NY, 2004, http://www.agsr-hichome.bnl.gov/AP/ap_notes/ap_note_149.pdf.
[7] X. Chang, Ph.D. thesis, Stony Brook University, 2005.
[8] J. van der Weide *et al.*, Phys. Rev. B **50**, 5803 (1994).
[9] J. Keister and J. Smedley, Nucl. Instrum. Methods Phys. Res., Sect. A **606**, 774 (2009).
[10] X. Chang *et al.*, in *Proceedings of 2005 Particle Accelerator Conference* (IEEE, Knoxville, Tennessee, 2005), p. 2711.
[11] J. Bohon, E. Muller, and J. Smedley, J. Synchrotron Radiat. **17** (2010).
[12] T. Watanabe *et al.*, J. Appl. Phys. **95**, 4866 (2004).
[13] G. Piantanida *et al.*, J. Appl. Phys. **89**, 8259 (2001).
[14] S. Hearne *et al.*, J. Appl. Phys. **99**, 113703 (2006).
[15] D. A. Dimitrov *et al.*, in *Proceedings of 2009 Particle Accelerator Conference* (IEEE, Report No. FR5PFP082-1/3, Vancouver, Canada, 2009).
[16] X. Chang *et al.*, in *Proceedings of 2007 Particle Accelerator Conference* (IEEE, Albuquerque, New Mexico, 2007), p. 2044.
[17] R. E. Thomas, R. A. Rudder, and R. J. Markunas, J. Vac. Sci. Technol. A **10**, 2451 (1992).